



**HAL**  
open science

# Unknown-Input Observer Design for Motorcycle Lateral Dynamics: TS Approach

Mohammed El-Habib Dabladji, Dalil Ichalal, Hichem Arioui, Saïd Mammar

► **To cite this version:**

Mohammed El-Habib Dabladji, Dalil Ichalal, Hichem Arioui, Saïd Mammar. Unknown-Input Observer Design for Motorcycle Lateral Dynamics: TS Approach. *Control Engineering Practice*, 2016, 54, pp.12–26. 10.1016/j.conengprac.2016.05.005 . hal-01317164

**HAL Id: hal-01317164**

**<https://hal.science/hal-01317164>**

Submitted on 18 May 2016

**HAL** is a multi-disciplinary open access archive for the deposit and dissemination of scientific research documents, whether they are published or not. The documents may come from teaching and research institutions in France or abroad, or from public or private research centers.

L'archive ouverte pluridisciplinaire **HAL**, est destinée au dépôt et à la diffusion de documents scientifiques de niveau recherche, publiés ou non, émanant des établissements d'enseignement et de recherche français ou étrangers, des laboratoires publics ou privés.

# Unknown-Input Observer Design for Motorcycle Lateral Dynamics: TS Approach

Mohammed El-Habib Dabladji, Dalil Ichalal, Hichem Arioui, and Saïd Mammam

## Abstract

In this paper, a nonlinear observer is designed in order to estimate the lateral dynamics of motorcycles. A nonlinear model of motorcycle's lateral dynamics is considered and is transformed in a Takagi-Sugeno (TS) exact form. An unknown input (UI) nonlinear observer is then designed in order to reconstruct the state variables whatever the forward velocity variations. The observer convergence study is based on the Lyapunov theory. The boundedness of the state estimation error is guaranteed thanks to the Input to State Stability (ISS) property. The observer has been tested on a nonlinear multibody model.

## Index Terms

Unknown input Observer, Two-Wheeled Vehicles, ISS, LMI.

## 1. INTRODUCTION

Riders are the most vulnerable drivers on road (20 times probability of fatal accidents). According to the latest statistics from the French Agency for Road Safety, the mortality rate for riders of powered single-track vehicles (PSTV) goes down more slowly than other types of vehicles (around 1%), which increases its share in total mortality, it is now approaching 24% (and 33% of injuries), for a part of 1.9% of road traffic [1]. This high rate mortality may be explained by several factors: first, motorcycles are inherently unstable; there are less typical safety systems for motorcycles and those developed for four-wheeled vehicles are not necessarily transferable for powered two-wheeled vehicles; finally, the motorcycle economic market is less interesting. In this context, several research projects have been initiated to address this need of preventive or active safety systems [2], [3].

The authors are with Informatique, Biologie Intégrative et Systèmes Complexes Laboratory, Evry Val d'Essonne University, 91020 Evry, France

E-mail: habib.dabladji@ibisc.univ-evry.fr

Fax: +33 1 69 47 06 03

To propose solutions to this problem, it is important to know the relevant variables governing motorcycle dynamics [4], [5]. This may be used later to know the maneuverability limits of these vehicles [6], [7] and to propose either warning preventive [2], [8] or active safety systems [9]. For example, several driver assistance systems like Anti-Lock and Combined Brake Systems (ABS/CBS) as well as Traction Control Systems (TCS) aim at the stability of motorcycles in order to improve the safety. However, the stability of motorcycles strongly depends on the roll angle. In this context, it is important to measure or estimate accurately this dynamic state. In fact, in some cases (curve warning), the limit velocity is depending on the roll angles and the lateral forces [10].

Consequently, during a bend, roll angle and lateral forces are important for the stability of motorcycles. These forces are necessary to guarantee the equilibrium of the vehicle when leaning and to stay into a turn (and avoid overturning or skidding situations). If the requested lateral forces exceed the tire-road friction (directly depend on the roll angles), the forces reach their saturation limit and the vehicle begins to skid sideways. In this context, it is important to estimate the lateral forces to know the limit of maneuverability of motorcycles and to avoid skidding.

However, the measurement by sensors of all states, inputs and parameters of the dynamics of motorcycle is inconceivable. Indeed, there are several variables that are difficult to measure for economic or technical reasons (steering torque, roll angle, pneumatic forces, road adherence, etc.). Thus, it is necessary to develop observers to estimate the states of motorcycle dynamics, to reconstruct rider's actions and to identify road features (slope, tilt, road adherence, etc.).

The state of the art of motorcycle observers is very limited. Indeed, the first observer estimating the roll angle of a motorcycle dates back to 2004 [11]. Several studies have been proposed for estimating the lateral dynamics; however, the steering dynamics has often been neglected: based on frequency separation filtering [12], [13], Kalman filtering [14], [15], PMI observer [16] or TS observer [17]. These techniques are developed under strict assumptions (neglect of the steering dynamics, neglect of tire-road contact, etc.) and another limitation is their lack of robustness with respect to changes in the longitudinal velocity.

The estimate of the steering angle was treated in [18] where a Linear Parameter Varying (LPV) observer has been proposed for the control of a semi-active steering system for different longitudinal velocities. However, the observer has been designed assuming a zero roll angle and no guarantee of convergence is given for variations in the roll angle.

The estimation of the longitudinal dynamics has been less treated. One can cite an interesting work [19], where an observer based controller using the Kalman filter has been proposed for the traction control.

To the best of our knowledge, the simultaneous estimation of the lateral dynamics, the lateral forces

and the steering dynamics was treated for the first time in [20] using the high order sliding mode techniques for a constant longitudinal velocity; However, it turned to be not robust to changes in the longitudinal velocity. An observer-based controller using TS techniques has been proposed in [21] under the assumption of knowledge of the steering torque, which is not obvious to measure.

The estimation of the lateral dynamics and lateral forces (without the knowledge of the steering torque) has not been previously treated for time-varying longitudinal speeds. To take into account the time variations in the longitudinal speed and some nonlinearities due to the high roll angle values, a nonlinear model of motorcycles is considered and expressed in a quasi-LPV one and then transformed into a Takagi-Sugeno (TS) form by following the sector nonlinearity approach [22]. This modelling approach is interesting because it may represent the behavior of the nonlinear system in a large domain of operating comparing to linear models. In addition, the simple structure of the TS models offers the possibility to extend some synthesis and analysis tools from the rich domain of linear systems to nonlinear ones: Lyapunov stability, Linear Matrix Inequalities (LMIs), etc. A nonlinear observer based on TS techniques was proposed in [23] to estimate the lateral and steering dynamics but without the validation on a motorcycle simulator or with real data. In addition, no robustness study was provided.

Based on the ISS property, a TS observer with UI decoupling is proposed to reconstruct the lateral dynamics of motorcycles for a wide range of longitudinal velocities. Using the ISS concept, the boundedness of the state estimation errors is proven. In addition, the result is formalized as an optimization problem under LMI constraints aiming to minimize the error bound for more accurate estimations.

The contributions of the paper are the following:

- The simultaneous estimation of the lateral dynamics and the lateral forces for time-varying longitudinal velocities.
- The estimation is ensured without the knowledge of the steering torque.
- Simulation results are given for different scenarios on the well-known simulator of motorcycles *BikeSim* based on the nonlinear multibody model of Sharp [4].

This paper is organized as follows: section II is dedicated to the motorcycle modeling, in section III, details of the proposed observer are given with the proof of the convergence of the motorcycle states. Finally, section IV provides some comparison results and discussions on the proposed observer.

## 2. MOTORCYCLE LATERAL DYNAMICS

This section highlights the different steps followed to obtain the TS model used by the observer. Firstly, from the model proposed by Sharp in 1971 [24], a quasi-LPV model is obtained and transformed into a TS model.

### 2..1. Nonlinear model

The most important dynamics of motorcycle can be decomposed into In-Plane and Out-Of-Plane dynamics [5]. The aim of this paper is the estimation of the Out-Of-Plane dynamics which consist on the lateral and steering ones.

In this paper, the Out-Of-Plane dynamics of the motorcycle are modeled as detailed in Sharp's 71 model [24]. The In-Plane dynamics are neglected and the longitudinal velocity is supposed constant or varying slowly (to neglect the coupling between the longitudinal and lateral dynamics). The vehicle is considered as a set of two rigid frames joined at the steering axis with freedom, restrained by a linear steering damper (figure 1).

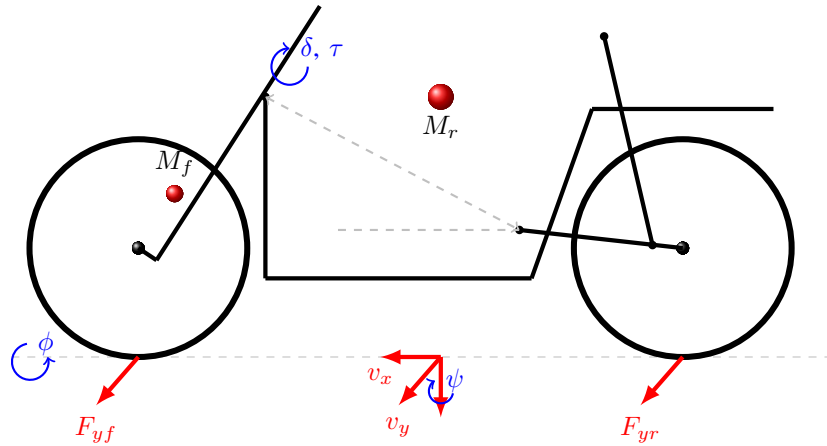


Fig. 1. Geometrical representation of the Sharp's motorcycle model

The main frame is subject to lateral motion, roll motion and yaw motion and the front frame is subject to steering motion. Thus, the obtained model has 4 degrees of freedom.

Considering the following assumptions:

*Assumption 1:*

- The aerodynamic forces are neglected.
- Movements due to the suspension are neglected.
- The rider is supposed rigidly attached to the main frame.

Under these assumptions, the motions of the motorcycle can be described by the following equations (with  $\dot{x}$  and  $\ddot{x}$  denote the first and second time-derivative of  $x$ ):

- Lateral motion

$$M(\dot{v}_y + \dot{\psi}v_x) + M_f k \ddot{\psi} + (M_f j + M_r h) \ddot{\phi} + M_f e \ddot{\delta} = F_{yf} + F_{yr} \quad (1)$$

- Yaw motion

$$M_f k (\dot{v}_y + \dot{\psi} v_x) + a_2 \ddot{\phi} + a_3 \ddot{\psi} + a_1 \ddot{\delta} - a_4 v_x \dot{\phi} - \frac{\dot{v}_y}{R_f} \sin(\epsilon) v_x \dot{\delta} = l_f F_{yf} - l_r F_{yr} \quad (2)$$

- Roll motion

$$(M_f j + M_r h) \dot{v}_y + b_2 \ddot{\phi} + a_2 \ddot{\psi} + b_1 \ddot{\delta} + b_5 v_x \dot{\psi} + \frac{\dot{v}_y}{R_f} \cos(\epsilon) v_x \dot{\delta} = b_4 \sin(\phi) - b_3 \sin(\delta) \quad (3)$$

- Steering motion

$$M_f e \dot{v}_y + b_1 \ddot{\phi} + a_1 \ddot{\psi} + c_1 \ddot{\delta} - \frac{\dot{v}_y}{R_f} \cos(\epsilon) v_x \dot{\phi} + c_3 v_x \dot{\psi} + K \dot{\delta} = -b_3 \sin(\phi) - c_2 \sin(\delta) - \eta F_{yf} + \tau \quad (4)$$

where the parameters defined in the above equations are similar to ones given in [24] and are listed in table I.

The lateral front and rear forces  $F_{yf}$  and  $F_{yr}$  are considered in their linear form with relaxation. Note that including the relaxation of the tire forces is important for the stability of the Sharp's model. Of course, the relaxation is important to take into account the wobble mode at high speeds [24]. The lateral forces are modeled by the following set of equations:

$$\begin{cases} \frac{\sigma_f}{v_x} \dot{F}_{yf} = -F_{yf} - C_{f1} \alpha_f + C_{f2} \gamma_f \\ \frac{\sigma_r}{v_x} \dot{F}_{yr} = -F_{yr} - C_{r1} \alpha_r + C_{r2} \gamma_r \end{cases} \quad (5)$$

where

$$\begin{cases} \alpha_f = \left( \frac{v_y + l_f \dot{\psi} - \eta \dot{\delta}}{v_x} \right) - \delta \cos(\epsilon) \\ \alpha_r = \left( \frac{v_y - l_r \dot{\psi}}{v_x} \right) \end{cases} \quad (6)$$

and

$$\begin{cases} \gamma_f = \phi + \delta \sin(\epsilon) \\ \gamma_r = \phi \end{cases} \quad (7)$$

Considering the lateral forces in their linear form is not restrictive because the addressed scenarios are limited to urban situations where the camber and slip angles remains in the linear domain of the lateral forces [25].

## 2.2. Quasi-LPV and TS models

In this subsection, the nonlinear model given in the subsection 2.1 will be transformed into a quasi-Linear Parameter Varying (quasi-LPV) structure and after to a Takagi-Sugeno (TS) model. The definitions of quasi-LPV and TS models can be found in [22], [26].

Now, from equations (1-7), the motorcycle lateral dynamics will be modeled by the following state space model:

$$E \dot{x}(t) = \mathcal{A}(v_x, \text{sinc}(\phi), \text{sinc}(\delta)) x(t) + \mathcal{B} \tau(t) \quad (8)$$

TABLE I  
MOTORCYCLE DYNAMICS VARIABLES

Motorcycle lateral dynamics parameters	
$v_x, v_y$	longitudinal and lateral velocities
$\phi, \psi, \delta$	roll, yaw and steering angles
$F_{yf}, F_{yr}$	front and rear lateral forces
$\tau$	steering torque
$M_f, M_r, M$	mass of the front frame, the rear frame and the whole motorcycle
$j, h, k, e, l_f, l_r$	linear dimensions (see Sharp's model [24])
$i_{fy}, i_{ry}$	polar moment of inertia of front and rear wheels
$R_f, R_r$	radius of front and rear wheels
$\epsilon$	caster angle
$K$	damper coefficient of the steering mechanism
$\eta$	mechanical trail
$I_{fx}, I_{rx}$	front and rear frame inertias about $X$ axis
$I_{fz}, I_{rz}$	front and rear frame inertias about $Z$ axis
$C_{rxz}$	rear frame product of inertia w.r.t. $X$ and $Z$ axis
$g$	acceleration due to gravity
$Z_f$	front vertical force
$C_{f1}, C_{r1}$	front and rear tire cornering stiffness
$C_{f2}, C_{r2}$	front and rear tire camber stiffness
$\sigma_f, \sigma_r$	coefficients of relaxation of the front and rear pneumatic forces
$\alpha_f, \alpha_r$	front and rear slip angles
$\gamma_f, \gamma_r$	front and rear camber angles
expressions of $a_i, b_i$ and $c_i$	
$a_1 = M_f ek + I_{fz} \cos(\epsilon), a_2 = M_f jk - C_{rxz} + (I_{fz} - I_{fx}) \sin(\epsilon) \cos(\epsilon), a_3 = M_f k^2 + I_{rz} + I_{fx} \sin^2(\epsilon) + I_{fz} \cos^2(\epsilon)$ $a_4 = -\left(\frac{i_{fy}}{R_f} + \frac{i_{ry}}{R_r}\right), b_1 = M_f ej + I_{fz} \sin(\epsilon), b_2 = M_f j^2 + M_r h^2 + I_{rx} + I_{fx} \cos^2(\epsilon) + I_{fz} \sin^2(\epsilon)$ $b_3 = \eta Z_f - M_f eg, b_4 = (M_f j + M_r h)g, b_5 = M_f j + M_r h + \frac{i_{fy}}{R_f} + \frac{i_{ry}}{R_r}, c_1 = I_{fz} + M_f e^2$ $c_2 = -(\eta Z_f - M_f eg) \sin(\epsilon), c_3 = M_f e + \frac{i_{fy}}{R_f} \sin(\epsilon)$	

where:  $x(t) = [\phi(t), \delta(t), v_y(t), \dot{\psi}(t), \dot{\phi}(t), \dot{\delta}(t), F_{yf}(t), F_{yr}(t)]^T$ .

$$E = \begin{bmatrix} 1 & 0 & 0 & 0 & 0 & 0 & 0 & 0 \\ 0 & 1 & 0 & 0 & 0 & 0 & 0 & 0 \\ 0 & 0 & M & e_{34} & e_{35} & e_{36} & 0 & 0 \\ 0 & 0 & e_{34} & e_{44} & e_{45} & e_{46} & 0 & 0 \\ 0 & 0 & e_{35} & e_{45} & e_{55} & e_{56} & 0 & 0 \\ 0 & 0 & e_{36} & e_{46} & e_{56} & e_{66} & 0 & 0 \\ 0 & 0 & 0 & 0 & 0 & 0 & 1 & 0 \\ 0 & 0 & 0 & 0 & 0 & 0 & 0 & 1 \end{bmatrix}, \mathcal{B} = \begin{bmatrix} 0 \\ 0 \\ 0 \\ 0 \\ 0 \\ 1 \\ 0 \\ 0 \end{bmatrix}$$

$$\text{and } \mathcal{A}(v_x, \text{sinc}(\phi), \text{sinc}(\delta)) = \begin{bmatrix} 0 & 0 & 0 & 0 & 1 & 0 & 0 & 0 \\ 0 & 0 & 0 & 0 & 0 & 1 & 0 & 0 \\ 0 & 0 & 0 & a_{34} \cdot v_x & 0 & 0 & 1 & 1 \\ 0 & 0 & 0 & a_{44} \cdot v_x & a_{45} \cdot v_x & a_{46} \cdot v_x & a_{47} & a_{48} \\ a_{51} \cdot \text{sinc}(\phi) & a_{52} \cdot \text{sinc}(\delta) & 0 & a_{54} \cdot v_x & 0 & a_{56} \cdot v_x & 0 & 0 \\ a_{61} \cdot \text{sinc}(\phi) & a_{62} \cdot \text{sinc}(\delta) & 0 & a_{64} \cdot v_x & a_{65} \cdot v_x & a_{66} & a_{67} & 0 \\ \\ a_{71} \cdot v_x & a_{72} \cdot v_x & a_{73} & a_{74} & 0 & a_{76} & a_{77} \cdot v_x & 0 \\ a_{81} \cdot v_x & 0 & a_{83} & a_{84} & 0 & 0 & 0 & a_{88} \cdot v_x \end{bmatrix}$$

The parameters  $a_{ij}$  and  $e_{ij}$  can easily be deduced from equations (1-7).  $\text{sinc}(x)$  is the cardinal sine function and is defined by:

$$\text{sinc}(x) = \begin{cases} 1 & \text{if } x = 0 \\ \frac{\sin(x)}{x} & \text{if } x \neq 0 \end{cases} \quad (9)$$

In the previous state-space model, the longitudinal velocity is considered as a linear varying parameter, because it is written in a linear form in the state matrix  $\mathcal{A}$ . The nonlinearity corresponding to the steering angle  $\sin(\delta)$  is approximated by  $\delta$  because of the low values of the steering angle (less than  $5^\circ$ ). The nonlinearities considered here are  $\text{sinc}(\phi)$  and  $v_x$ .

Since  $E$  is non-singular and under the assumption of low values of the steering angle, the model given by equation (8) can be written in a quasi-LPV form as follows:

$$\dot{x}(t) = A(\rho)x(t) + B\tau(t) \quad (10)$$

where:  $\rho = (v_x, \text{sinc}(\phi))^T$ ,  $A(\rho) = E^{-1}\mathcal{A}(v_x, \text{sinc}(\phi), 1)$ ,  $B = E^{-1}\mathcal{B}$

From the well-known sector nonlinearity approach [22], the quasi-LPV model can be written in an exact TS representation with 4 sub-models (because, there are 2 varying parameters). Indeed, the scheduling variables, also called premise variables in TS systems, are:

$$z_1 = v_x, \quad z_2 = \text{sinc}(\phi) \quad (11)$$

The longitudinal velocity is considered time-varying from  $v_{min}$  to  $v_{max}$  and the roll angle is considered having a maximal value  $\phi_{max}$ . Indeed, the bounds of the premise variables are:

$$v_{min} \leq z_1 \leq v_{max}, \quad \text{sinc}(\phi_{max}) \leq z_2 \leq 1 \quad (12)$$

From the well-known sector nonlinearity approach, a TS model is obtained as follows:

$$\dot{x}(t) = \sum_{i=1}^4 \mu_i(\rho) A_i x(t) + B\tau(t) \quad (13)$$

where:  $A_i = A(\rho_i)$ , and  $\rho_1 = (v_{min}, 1)^T$ ,  $\rho_2 = (v_{max}, 1)^T$ ,  $\rho_3 = (v_{min}, \phi_{max})^T$  and  $\rho_4 = (v_{max}, \phi_{max})^T$ .

The variables  $\mu_i(\rho)$  are called the weighing functions and they must satisfy the following convex sum property:

$$\begin{cases} 0 \leq \mu_i(v_x, \text{sinc}(\phi)) \leq 1 \\ \sum_{i=1}^4 \mu_i(v_x, \text{sinc}(\phi)) = 1 \end{cases} \quad (14)$$

The variables  $\mu_i(\rho)$  are computed as follows:

$$\begin{cases} h_{11} = \frac{v_{max} - z_1}{v_{max} - v_{min}} & , & h_{12} = \frac{z_1 - v_{min}}{v_{max} - v_{min}} \\ h_{21} = \frac{z_2 - \text{sinc}(\phi_{max})}{1 - \text{sinc}(\phi_{max})} & , & h_{22} = \frac{1 - z_2}{1 - \text{sinc}(\phi_{max})} \end{cases} \quad (15)$$

$$\begin{cases} \mu_1 = h_{11} \cdot h_{21} & , & \mu_2 = h_{12} \cdot h_{21} \\ \mu_3 = h_{11} \cdot h_{22} & , & \mu_4 = h_{12} \cdot h_{22} \end{cases} \quad (16)$$

In most cases, the roll and yaw rates are considered measurable thanks to gyroscopic sensors. The longitudinal velocity is also measurable. The steering angle and its time-derivative can be obtained with optical sensors. Moreover, conventional accelerometers allow us to measure the lateral acceleration which corresponds to the sum of lateral forces divided by the mass of the vehicle and the rider as follows:  $Ma_y = F_{yf} + F_{yr}$ .

Indeed, the measurements' vector is given by the following equation:

$$\begin{aligned} y(t) &= [\delta(t), \dot{\psi}(t), \dot{\phi}(t), \dot{\delta}(t), a_y]^T \\ &= [\delta(t), \dot{\psi}(t), \dot{\phi}(t), \dot{\delta}(t), \frac{(F_{yf} + F_{yr})}{M}]^T \\ &= Cx(t) \end{aligned} \quad (17)$$

$$\text{with: } C = \begin{bmatrix} 0 & 1 & 0 & 0 & 0 & 0 & 0 & 0 \\ 0 & 0 & 0 & 1 & 0 & 0 & 0 & 0 \\ 0 & 0 & 0 & 0 & 1 & 0 & 0 & 0 \\ 0 & 0 & 0 & 0 & 0 & 1 & 0 & 0 \\ 0 & 0 & 0 & 0 & 0 & 0 & \frac{1}{M} & \frac{1}{M} \end{bmatrix}$$

*Remark 1:* The observer will be designed on the use of the Sharp's 71 model according to some simplifications, like neglecting the suspension and assuming only very low accelerations. If these simplifications are not satisfied, the model will have more nonlinearities and additional states. This case may make the optimization problem under LMI constraints more difficult to solve. The observer will be designed based on ISS construction and its robustness towards many of these modeling imperfections will be studied in section 3.3.

*Remark 2:* In comparison to [21], in the present manuscript the relaxation of the tire forces is included. The relaxation allows to take into account some characteristics associated with high speeds like the wobble

mode [24]. In addition, from a theoretical point of view, if the relaxation of the tire forces is included, the nonlinearity  $\frac{1}{v_x}$  in the quasi-LPV model vanishes and a model with 2 nonlinearities will be obtained instead of 3 in [21]. Consequently, the TS model will have ( $2^2 = 4$ ) sub-models instead of ( $2^3 = 8$ ) and the optimization problem under LMI constraints will be less conservative.

*Remark 3:* The accelerometers and gyroscopes mounted on motorbikes measure the accelerations and the angular rates of the body-fixed frame of the vehicle. Consequently, the real accelerations and angular rates will be affected by the roll angle. If the effect of the roll angle in the measure of the acceleration and the angular rates is considered, the vector of measures ( $y(t) = C(\rho)x(t)$ ) will be nonlinear (coupled with other states). Consequently, the output matrix  $C(\rho)$  must be considered in a quasi-LPV form and it will be more difficult to satisfy the equality (41) in what follows. This issue has not been addressed in the proposed work and authors may refer to [27] for the observation of such systems.

If the pitch angle is neglected, the accelerations given by the accelerometer in the Y and Z axis in the body-fixed with respect to the real accelerations can be approximated by:

$$\begin{aligned} a_{ybf} &= a_y \cos \phi - g \sin \phi \\ a_{zbf} &= -a_y \sin \phi - g \cos \phi \end{aligned} \quad (18)$$

In what follows, when body-fixed sensors are considered, the lateral acceleration is approximated by:

$$a_y = \text{sign}(a_{ybf}) \sqrt{|a_{ybf}^2 + a_{zbf}^2 - g^2|} \quad (19)$$

### 3. OBSERVER DESIGN

In the design of the proposed observer, the ISS property is used and defined as:

*Definition 1:* [28] Given a system:

$$\dot{x}(t) = f(x(t), w(t)) \quad (20)$$

The system (20) verifies the ISS if there exists a  $\mathcal{KL}$  function  $\beta_{\mathcal{KL}} : \mathbb{R}^n \times \mathbb{R} \rightarrow \mathbb{R}$  and a  $\mathcal{K}$  function  $\beta_{\mathcal{K}} : \mathbb{R} \rightarrow \mathbb{R}$  such that for each input  $w(t)$  satisfying  $\|w(t)\|_{\infty} < \infty$  and each initial conditions  $x(0)$ , the trajectory of (20) associated to  $x(0)$  and  $w(t)$  satisfies

$$\|x(t)\|_2 \leq \beta_{\mathcal{KL}}(\|x(0)\|, t) + \beta_{\mathcal{K}}(\|w(t)\|_{\infty}) \quad (21)$$

Class  $\mathcal{KL}$  and  $\mathcal{K}$  functions are as defined in [29].

The proposed paper deals with the Unknown Input (UI) observers for quasi-LPV systems written in a TS form. In this context, the ISS property will be formulated as an optimization problem under LMI conditions. The following lemma is used in the proof of the observer convergence study.

*Lemma 1:* Consider the continuous-time TS system:

$$\begin{cases} \dot{x}(t) &= \sum_{i=1}^r \mu_i(\rho)(A_i x(t) + B_i u(t)) \\ &= A(\rho)x(t) + B(\rho)u(t) \end{cases} \quad (22)$$

The system (22) verifies the following ISS property with the minimal ISS gain  $\varphi_2$ :

$$\|x(t)\|_2 \leq \varphi_1 \cdot \|x(0)\|_2 e^{-\frac{\alpha t}{2}} + \varphi_2 \cdot \|u(t)\|_\infty \quad (23)$$

if there exist positive scalars  $\alpha$  and  $\gamma$  and a symmetric positive definite matrix  $Q$  with minimal and maximal Eigenvalues  $\chi_1$  and  $\chi_2$  such that the following optimization problem under LMI conditions is satisfied for  $i = 1, \dots, r$ :

$$\min_{Q, M_i, \gamma} \gamma \quad (24)$$

s.t.

$$\chi_1 I \leq Q \quad (25)$$

$$\begin{bmatrix} A_i^T Q + Q A_i + \alpha P & Q B_i \\ B_i^T Q & -\gamma I \end{bmatrix} < 0 \quad (26)$$

with  $\varphi_1 = \sqrt{\frac{\chi_2}{\chi_1}}$ ,  $\varphi_2 = \sqrt{\frac{\gamma}{\alpha \chi_1}}$  and  $\chi_1 I \leq Q \leq \chi_2 I$

LMI conditions (25, 26) are sufficient to satisfy the ISS property, and the minimization of  $\gamma$  in (24) allows the minimization of the ISS gain  $\varphi_2$ .

The procedure to solve this optimization problem begins by imposing  $\alpha$  and  $\chi_1$  and solving the optimization problem (24) under the LMI conditions (25, 26). If, no solution is found, one has to decrease  $\alpha$  or  $\chi_1$ .

*Proof:* By considering the following Lyapunov function:

$$V(t) = x(t)^T Q x(t) \quad (27)$$

$V(t)$  is a Lyapunov function means that  $V(t)$  can be bounded as follows:

$$\chi_1 \cdot \|x(t)\|_2^2 \leq V(t) \leq \chi_2 \cdot \|x(t)\|_2^2 \quad (28)$$

where  $\chi_1$  and  $\chi_2$  are the minimal and maximal Eigenvalues of the matrix  $Q$ . Hence, the inequality (25) must be checked to impose a minimal eigenvalue to the matrix  $Q$ .

From the state system (22), by differentiating the Lyapunov (27) w.r.t. time, one obtains:

$$\begin{aligned}\dot{V}(t) &= x(t)^T (QA(\rho) + A(\rho)^T Q) x(t) + 2x(t)^T QB(\rho)u(t) \\ &= \begin{bmatrix} x(t) \\ u(t) \end{bmatrix}^T \begin{bmatrix} QA(\rho) + A(\rho)^T Q + \alpha Q & QB \\ B^T Q & -\gamma I \end{bmatrix}^T \begin{bmatrix} x(t) \\ u(t) \end{bmatrix} - \alpha x(t)^T Q x(t) + \gamma u(t)^T u(t)\end{aligned}\quad (29)$$

If the inequality (26) is satisfied for all  $1 \leq i \leq r$ , then the time-derivative of the Lyapunov function will be bounded as follows:

$$\begin{aligned}\dot{V}(t) &< -\alpha x(t)^T Q x(t) + \gamma u(t)^T u(t) \\ &= -\alpha V(t) + \gamma u(t)^T u(t)\end{aligned}\quad (30)$$

By integrating the last inequality w.r.t. from 0 to  $t$ , it follows:

$$\begin{aligned}V(t) &< V(0)e^{-\alpha t} + \gamma \int_0^t e^{-\alpha(t-s)} \|u(s)\|_2^2 ds \\ &\leq V(0)e^{-\alpha t} + \frac{\gamma}{\alpha} \|u(t)\|_\infty^2\end{aligned}\quad (31)$$

Now, thanks to the inequality (28), one obtains:

$$\|x(t)\|_2^2 < \frac{\chi_2}{\chi_1} \|x(0)\|_2^2 e^{-\alpha t} + \frac{\gamma}{\alpha \chi_1} \|u(t)\|_\infty^2\quad (32)$$

The last inequality is equivalent to:

$$\|x(t)\|_2 < \sqrt{\frac{\chi_2}{\chi_1}} \|x(0)\|_2 e^{-\frac{\alpha t}{2}} + \sqrt{\frac{\gamma}{\alpha \chi_1}} \|u(t)\|_\infty\quad (33)$$

This inequality proves the ISS property of the system (22).

Since  $\alpha$  and  $\chi_1$  are imposed before solving the LMI problem, the minimization of  $\gamma$  will ensure the minimal bound of the ISS gain between the perturbation input  $u(t)$  and the state vector  $x(t)$ .

Note that the ISS property is stronger than other stability properties like  $\mathcal{L}_2$  stability or the ISpS [30].

■

### 3.1. Observer structure

The objective of this section is to design an UI observer in order to reconstruct the lateral dynamics of the motorcycle. The nonlinear observer has a quasi-LPV structure as well as the motorcycle lateral dynamics model. The main two difficulties in the design of the observer are the lack of knowledge of rider's torque and the fact that the scheduling variables are partially unmeasurable.

In this context, the following nonrestrictive assumptions are considered:

*Assumption 2:* In what follows, it is supposed that:

- the state vector  $x(t)$  and the input steering torque  $\tau(t)$  are considered bounded (stabilized motorcycle case),
- $\text{rank}(CB) = \text{rank}(B)$ ,
- the pair  $(A(\rho), C)$  is observable for all  $\rho \in ([v_{min}, v_{max}] \times [-\phi_{max}, \phi_{max}]) \subset \mathbb{R}^2$ .

The first assumption holds in open-loop for a some longitudinal velocities [24] and the motorcycle is also assumed to be under rider control. The second and the third assumptions can easily be checked numerically.

Let us consider the following nonlinear observer [31]:

$$\begin{cases} \dot{z}(t) &= N(\hat{\rho})z(t) + L(\hat{\rho})y(t) \\ \hat{x}(t) &= z(t) - Hy(t) \end{cases} \quad (34)$$

The vector  $\hat{\rho} = (\hat{v}_x, \hat{\phi})^T$  may be different from  $\rho$  because the roll angle  $\phi$  is not measured and the longitudinal velocity  $v_x$  may be affected by noises and perturbations.  $\hat{v}_x$  is the measured longitudinal velocity obtained by a suitable sensor and  $\hat{\phi}$  is the roll angle obtained from the observer. The matrices  $N(\hat{\rho}) \in \mathbb{R}^{n \times n}$ ,  $L(\hat{\rho}) \in \mathbb{R}^{n \times n_y}$ ,  $H \in \mathbb{R}^{n \times n_y}$  of the observer are to be determined in such a way to have the minimal bound of the estimation errors.  $n$  and  $n_y$  are the dimensions of the state vector and the output vector.

$N(\hat{\rho})$  and  $L(\hat{\rho})$  have the same quasi-LPV form as the matrix  $A(\rho)$  and may be written in a TS form as follows:

$$N(\hat{\rho}) = \sum_{i=1}^r \mu_i(\hat{\rho})N_i, \quad L(\hat{\rho}) = \sum_{i=1}^r \mu_i(\hat{\rho})L_i \quad (35)$$

In what follows, it will be assumed that the weighing functions  $\mu_i(\hat{v}_x, \hat{\phi})$  always satisfy the conditions given in (14). This assumption holds if the longitudinal velocity given by the sensor is considered between the bounds  $v_{min}$  and  $v_{max}$  given for the TS system. Moreover, the  $\text{sinc}(\cdot)$  function can always be bounded.

One can note that the proposed observer has been chosen for its simplicity. Others structures of UI observers with adaptation of the UI estimation have been proposed. However, for non-constant UI, conventional TS-PI (Proportional Integrator) type observers are not efficient, because the UI must be constant [32]. Another structure of UI observer has been proposed in [23] with a PD adaptation law of the UI. The proposed observer leads to easier LMIs constraints to solve compared to [23] because there are fewer variables to be determined in the optimization problem. Also, in [23], there was an LME condition ( $BP = F^T C$ ) combined with the LMI constraints. In the proposed work, the LME conditions

are solved in a first step independently from the optimization problem under LMI constraints. Moreover, the estimation error obeys to the ISS property, which is stronger than ISpS property obtained in [23].

According to equations (17, 34), the state estimation error is given by:

$$e = x - \hat{x} = \underbrace{(I + HC)}_P x - z \quad (36)$$

From equations (10, 34, 36), the state estimation error obeys to the following differential equation:

$$\begin{aligned} \dot{e}(t) &= PA(\rho)x(t) + PB\tau(t) - N(\hat{\rho})z(t) - L(\hat{\rho})Cx(t) \\ &= N(\hat{\rho})e(t) + (PA(\hat{\rho}) - N(\hat{\rho})P - L(\hat{\rho})C)x(t) + PB\tau(t) + P\zeta(t) \end{aligned} \quad (37)$$

with  $\zeta(t) = (A(\rho) - A(\hat{\rho}))x(t)$

### 3..2. Observer design and convergence study

Under the conditions:

$$PB = 0 \quad (38)$$

$$PA(\hat{\rho}) - N(\hat{\rho})P - L(\hat{\rho})C = 0 \quad (39)$$

the estimation error dynamics will be reduced to:

$$\dot{e}(t) = N(\hat{\rho})e(t) + P\zeta(t) \quad (40)$$

Thanks to lemma 1, ISS performances can be obtained for the system (40). To obtain the observer gains that satisfy the LME conditions (38, 39) and minimize the ISS gain between the perturbation vector  $\zeta(t)$  and the estimation error's vector  $e(t)$  for the system (40), the following steps in the design approach are followed.

First, the equality (38) leads to:

$$\begin{aligned} (I + HC)B = 0 &\Leftrightarrow HCB = -B \\ &\Leftrightarrow H = -B(CB)^+ \end{aligned} \quad (41)$$

where:  $(CB)^+ = [(CB)^T(CB)]^{-1}(CB)^T$  is the left pseudo-inverse of the matrix  $(CB)$ .

After computing the matrix  $H$ , the matrix  $P$  is computed and replaced in the equality (39) which leads to:

$$\begin{aligned} PA(\hat{\rho}) - N(\hat{\rho})(I + HC) - L(\hat{\rho})C = 0 &\Leftrightarrow \underbrace{PA(\hat{\rho}) - N(\hat{\rho})}_{\Gamma(\hat{\rho})} - \underbrace{(N(\hat{\rho})H + L)}_{K(\hat{\rho})}C = 0 \\ &\Leftrightarrow N(\hat{\rho}) = \Gamma(\hat{\rho}) - K(\hat{\rho})C \end{aligned} \quad (42)$$

Then, the state estimation error's dynamics become:

$$\dot{e}(t) = (\Gamma(\hat{\rho}) - K(\hat{\rho})C)e(t) + P\zeta(t) \quad (43)$$

From assumption 2, the term  $\zeta(t)$  is assumed bounded and will be seen in what follows as a perturbation whose effect will be minimized.

Then, thanks to lemma 1 and to the boundedness of  $\zeta(t)$ , if there exists a positive definite matrix  $Q$ , matrices  $K_i$  and positive scalars  $\alpha$ ,  $\chi_1$  and  $\gamma$  such that for all  $1 \leq i \leq r$ :

$$\begin{bmatrix} (\Gamma_i - K_i C)^T Q + Q(\Gamma_i - K_i C) + \alpha Q & QP \\ P^T Q & -\gamma I \end{bmatrix} < 0 \quad (44)$$

and

$$Q \geq \chi_1 I \quad (45)$$

then, the system (43) is stable and verifies the ISS property:

$$\|e(t)\|_2 \leq \varphi_1 \|e(0)\|_2 e^{-\frac{\alpha t}{2}} + \varphi_2 \|\zeta(t)\|_\infty \quad (46)$$

with  $\varphi_1 = \sqrt{\frac{\chi_2}{\chi_1}}$ ,  $\varphi_2 = \sqrt{\frac{\gamma}{\alpha\chi_1}}$  and  $\chi_1 I \leq Q \leq \chi_2 I$

By considering  $M_i = QK_i$ , the LMI condition (44) will be equivalent to the following:

$$\begin{bmatrix} \Gamma_i^T Q + Q\Gamma_i - C^T M_i^T - M_i C + \alpha Q & QP \\ P^T Q & -\gamma I \end{bmatrix} < 0 \quad (47)$$

In order to minimize the ISS gain from the perturbation term  $\zeta(t)$  to the vector of estimation errors  $e(t)$ , the matrices  $K_i$  and  $Q$  must be computed in order to minimize the ISS gain:  $\varphi_2 = \sqrt{\frac{\gamma}{\alpha\chi_1}}$ . Since  $\alpha$  and  $\chi_1$  are imposed before solving the optimization problem, the minimization of  $\varphi_2$  is equivalent to the minimization of  $\gamma$ .

The UI observer design procedure is summarized in the following steps:

- 1) verify the observability condition of the couple  $(A(\rho), C)$  and the rank condition ( $\text{rank}(CB) = \text{rank}(B)$ ).
- 2) compute the matrices  $H$  and  $P$  as follows:

$$\begin{cases} H = -B(CB)^+ \\ P = I + HC \end{cases} \quad (48)$$

- 3) for some positive scalars  $\alpha$  and  $\chi_1$ , solve the optimization problem under LMI conditions given by:

$$\min_{Q, M_i, \gamma} \gamma \quad (49)$$

s.t.

$$Q \geq \chi_1 I \quad (50)$$

$$\begin{bmatrix} \Gamma_i^T Q + Q \Gamma_i - C^T M_i^T - M_i C + \alpha Q & QP \\ P^T Q & -\gamma I \end{bmatrix} < 0 \quad (51)$$

with  $\Gamma_i = PA_i$

- 4) if the optimization problem does not accept a numerical solution, decrease  $\alpha$  or  $\chi_1$  and repeat the optimization problem under LMI constraints; else, go to the next step.
- 5) the gains of the observer  $N(\hat{\rho})$  and  $L(\hat{\rho})$  are computed as follows:

$$\begin{aligned} M(\hat{\rho}) &= \sum_{i=1}^r \mu_i(\hat{\rho}) M_i \\ \Gamma(\hat{\rho}) &= \sum_{i=1}^r \mu_i(\hat{\rho}) \Gamma_i \\ K(\hat{\rho}) &= Q^{-1} M(\hat{\rho}) \\ N(\hat{\rho}) &= \Gamma(\hat{\rho}) - K(\hat{\rho}) C \\ L(\hat{\rho}) &= K(\hat{\rho}) - N(\hat{\rho}) H \end{aligned} \quad (52)$$

This ends the steps of the observer's design.

### 3.3. Observer robustness study

In the previous subsection, motorcycle's parameters have been considered well known and the observer was designed on the use of the Sharp's 71 model according to some simplifications. What about the robustness of the observer if the model parameters are not exactly known or if the modeling simplifications are not satisfied? In this case, the model of the motorcycle's lateral dynamics may be written as follow:

$$\dot{x}(t) = (A(\rho) + \Delta A(\rho))x(t) + (B + \Delta B)u(t) \quad (53)$$

Now, let us consider the following observer:

$$\begin{cases} \dot{z}(t) &= N(\hat{\rho})z(t) + L(\hat{\rho})y(t) \\ \hat{x}(t) &= z - Hy(t) \end{cases} \quad (54)$$

The estimation error is always the same:

$$e = x - \hat{x} = \underbrace{(I + HC)}_P x - z \quad (55)$$

Then, the estimation error's dynamics becomes:

$$\dot{e}(t) = N(\hat{\rho})e(t) + (PA(\hat{\rho}) - N(\hat{\rho})P - L(\hat{\rho})C)x(t) + PBu(t) + P\zeta_1(t) \quad (56)$$

with  $\zeta_1(t) = (A(\rho) - A(\hat{\rho}))x(t) + \Delta A(\rho)x(t) + \Delta Bu(t) = \zeta(t) + \Delta A(\rho)x(t) + \Delta Bu(t)$

The estimation errors' dynamic (56) is similar to that obtained in the previous subsection in equation (37). The difference lies in the perturbation vector  $\zeta_1(t)$  which includes the uncertainties on the matrix  $A(\rho)$  and  $B$ . Then, the same previous study is performed in this case and the ISS performances are always fulfilled.

In the nominal case where the parameters are considered exactly known, the estimation error was bounded as follows:

$$\|e(t)\|_2 \leq \varphi_1 \|e(0)\|_2 e^{-\frac{\alpha t}{2}} + \varphi_2 \|\zeta(t)\|_\infty \quad (57)$$

By analogy, in the uncertain case, the estimation error will be bounded as follows:

$$\begin{aligned} \|e(t)\|_2 &\leq \varphi_1 \|e(0)\|_2 e^{-\frac{\alpha t}{2}} + \varphi_2 \|\zeta_1(t)\|_\infty \\ &\leq \varphi_1 \|e(0)\|_2 e^{-\frac{\alpha t}{2}} + \varphi_2 (\|\zeta(t)\|_\infty + \|\Delta A(\rho)x(t) + \Delta B u(t)\|_\infty) \end{aligned} \quad (58)$$

When  $t \rightarrow \infty$ , the estimation error will be bounded by the quantity  $\varphi_2 \|\zeta(t)\|_\infty$ , in the nominal case, and by the quantity  $\varphi_2 (\|\zeta(t)\|_\infty + \|\Delta A(\rho)x(t) + \Delta B u(t)\|_\infty)$ , in the uncertain case. Consequently, the accuracy of the observer will be better in the nominal case because the bounds of convergence are smaller.

#### 4. RESULTS OF SIMULATION

The gains of the UI observer are computed from the equations (48 - 52) applied to the TS model given in subsection II-B, where the numerical values of the matrices  $E$ ,  $A$  and  $B$  are given in the annex. In the optimization problem, the longitudinal velocity is considered varying from:  $v_{min} = 30km/h$  to  $v_{max} = 120km/h$  and the maximal roll angle:  $\phi_{max} = \pi/5 rad$ . The parameters used in the optimization problem are chosen as follows:  $\alpha = 1$ ,  $\chi_1 = 10^{-6}$ . The optimization problem under LMI and LME conditions is solved using Yalmip toolbox under Matlab. The obtained ISS gain is about  $\varphi_2 = \sqrt{\frac{\gamma}{\alpha\chi_1}} = 0.2229$ . The simulations are carried out on the well-known motorcycle's simulator: *BikeSim* based on the nonlinear multibody Sharp's 2004 model [4].

For safety purposes and ADAS design, it is more interesting to estimate the lateral forces and the roll angle rather than the steering dynamics. These states are considered as the main pertinent lateral variables and only their estimations will be displayed in this paper.

Firstly, simulations are given for a double lane change maneuver and for different longitudinal velocities profiles. After, a scenario of 70s on 3km with a variable longitudinal velocity and lateral motions is considered.

For a double lane change maneuver with a velocity of  $v_x = 100km/h$ , the results are depicted in figure 2. For the same maneuver with a velocity of  $v_x = 50km/h$ , results of simulation are given in

figure 3. For a double lane change maneuver under braking, the results are depicted in figure 4. The steering angle and its estimation for the three scenarios are depicted in the figure 5.

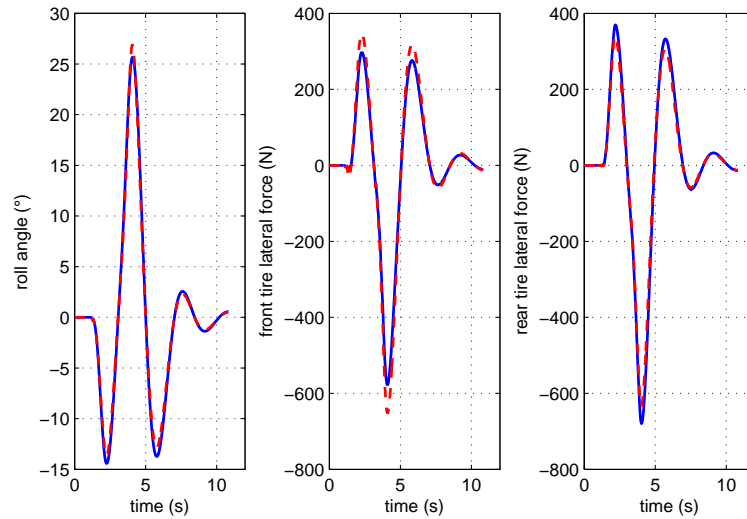


Fig. 2. Double lane change at  $100\text{km}/h$ . In blue: nonlinear multibody model and in red: estimation results.

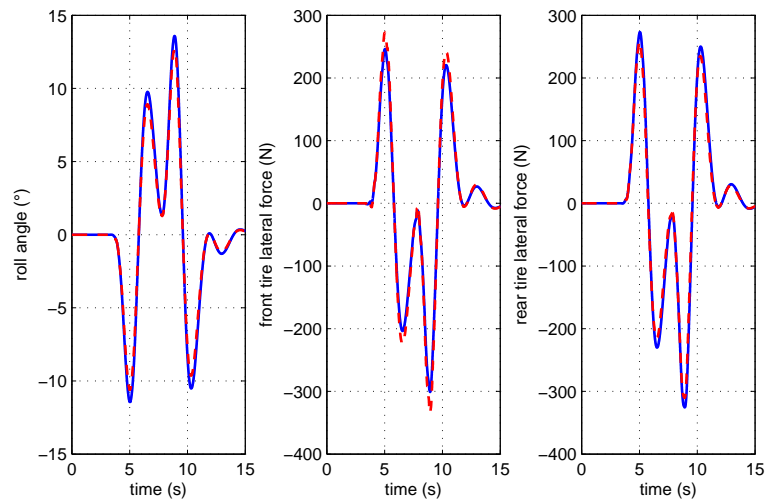


Fig. 3. Double lane change at  $50\text{km}/h$ . In blue: nonlinear multibody model and in red: estimation results.

Note that in the three scenarios, the roll angle and the lateral forces are well estimated. Of course, there are some differences at the peak of the roll angle and the forces. This can be explained by modeling errors due to linearization. The model used for the observer design does not take into account large roll

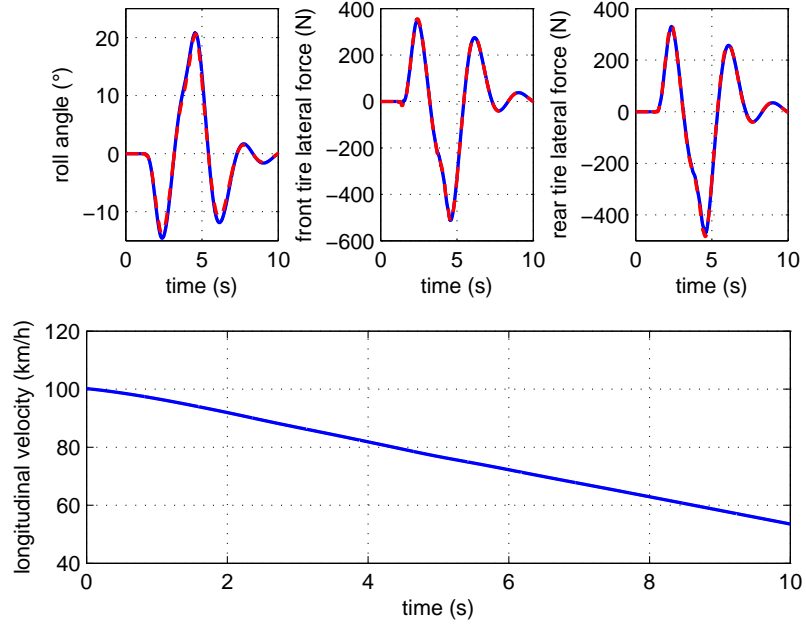


Fig. 4. Double lane change with braking from  $v_x = 100\text{km/h}$  to  $v_x = 50\text{km/h}$ . Top: in blue nonlinear multibody model and in red estimation results. Bottom: longitudinal velocity profile

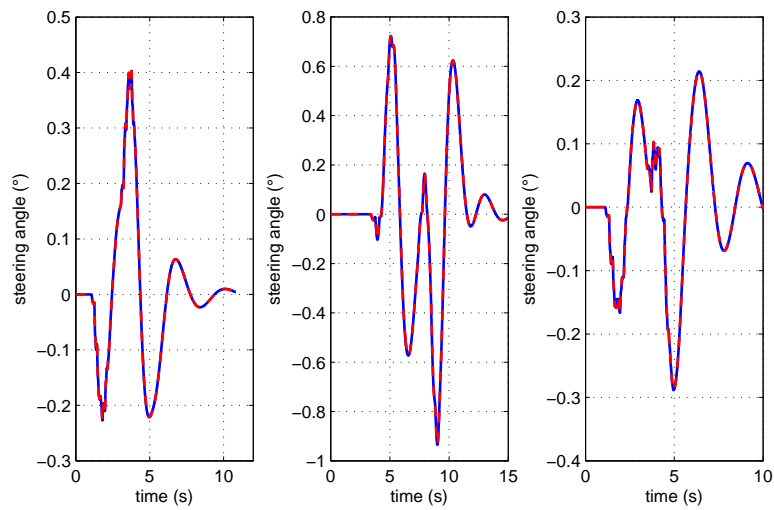


Fig. 5. Steering angle and its estimation for: (left) 1<sup>st</sup> scenario at  $100\text{km/h}$ , (center) 2<sup>nd</sup> scenario at  $50\text{km/h}$  and (right) 3<sup>rd</sup> scenario with braking. In blue: steer angle and in red: its estimation

angles. However, it still gives acceptable results in these situations. Moreover, even for a braking scenario where the Sharp's 71 model is not valid (the model does not take into account the longitudinal dynamics or velocity variation), the simulation results remain acceptable.

*Remark 4:* The Sharp's 71 model is a pure lateral motion model valid for different constant longitudinal velocities. Indeed, the Sharp's 71 model do not take into account the longitudinal dynamics (velocity variation). Of course, when accelerating or braking, other dynamics associated with the longitudinal motions appear such as the load transfer between the two tires, the motions of the suspension and the saturation of the lateral forces [4], [5].

In this context, the model used for the observer design is not valid for acceleration or braking. Under this limitation, good performances of the observer are still preserved.

Now, to assess the performances of the observer, the normalized error  $\epsilon_z$  is computed for the estimation of the different variables. The normalized error for a variable  $z$  is given by [33]:

$$\epsilon_z = \frac{100(\|z_{mes} - z_{est}\|)}{\max \|z_{mes}\|} \quad (59)$$

where  $z_{mes}$  is the measurement of  $z$  and  $z_{est}$  is its estimate provided by the observer.

The table II presents the maximum, the mean and the variance of the normalized errors for the different scenarios.

TABLE II

NORMALIZED ERROR FOR A DOUBLE LANE CHANGE AND DIFFERENT VELOCITIES. (A)  $v_x = 100km/h$ , (B)  $v_x = 50km/h$ , (C) BRAKING FROM  $100km/h$  TO  $60km/h$

	roll angle			front lateral force			rear lateral force		
	(A)	(B)	(C)	(A)	(B)	(C)	(A)	(B)	(C)
max( $\epsilon_z$ ) (%)	5.42	8.52	5.94	12.87	11.23	2.43	8.57	9.20	4.17
mean( $\epsilon_z$ ) (%)	1.49	2.24	1.90	3.06	2.42	0.50	1.91	1.98	1.04
std( $\epsilon_z$ ) (%)	1.52	2.60	1.76	3.58	2.98	0.51	2.23	2.50	1.03

In all the scenarios, the means of the normalized error for the roll angle and the lateral forces are less than 4%. So, it can be said that the estimation of the roll angle and lateral forces are good even under soft acceleration.

Next, the robustness of the observer to the uncertainties in the longitudinal velocity is tested. A scenario of a constant longitudinal velocity of  $100km/h$  in a double lane change is considered. But, the observer will be excited with a different constant longitudinal velocity ( $v_x = 90km/h$ ). In this case, the results are given in figure 6. Despite modeling and longitudinal velocity uncertainties, the estimation error dynamics

still have ISS performances and the observer ensures a good estimation of the roll angle and the lateral forces.

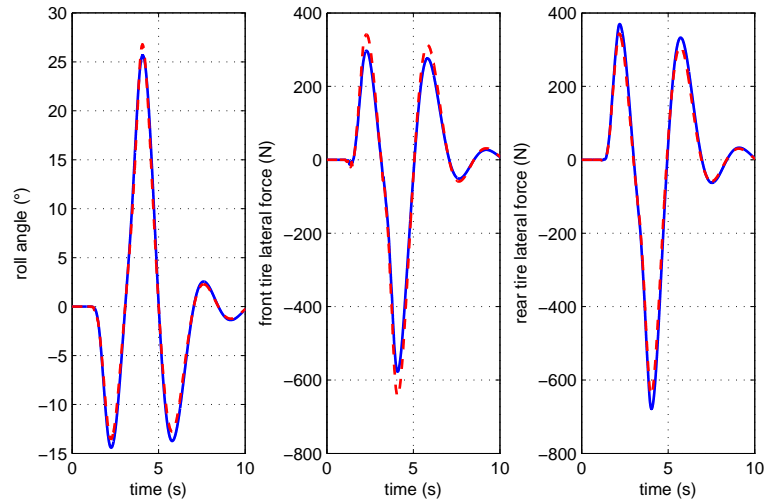


Fig. 6. Double lane change at  $100km/h$ . In blue: nonlinear multibody model, in red: estimation results with the false longitudinal velocity  $v_x = 90km/h$ .

The robustness of the observer to the parameters uncertainties is now tested. To this end, the mass of the vehicle and the rider are increased by  $46kg$  equivalent to an increase of 17% and the caster angle is decreased by 10%. The results of simulation are given in figure 7. From simulation results, one can state that the performances of the observer are preserved even in the presence of parametric uncertainties.

The robustness of the observer is also tested with respect to uncertainties in the road friction coefficient. To this end, two cases for the double lane change maneuver at  $100km/h$  are considered and compared. In the first case, the road friction coefficient varies suddenly from  $\beta = 1$  (dry asphalt) to 0.7 (moderately wet road); and in the second case, it varies from  $\beta = 0.7$  to 0.4 (very wet road). The results of roll angle estimation are given in figures 8 and 9 and the maximum, the mean and the variance of normalized estimation errors are given for the roll angle and the lateral forces in table III.

Remind that the observer was designed using Sharp's 1971 model where the tire coefficients  $C_{fi}$  and  $C_{ri}$  were computed for a nominal case with  $\beta = 0.85$ . From figure 8, the effect of the sudden variation of the road friction coefficient is more notable for the second case from  $t = 3.6s$ . Indeed, in the first case, the road friction coefficient varies from  $\beta = 1$  to  $\beta = 0.7$  which are close to the coefficient used for the observer design ( $\beta = 0.85$ ). However, the road friction coefficient in the second case is much more different from the nominal road friction coefficient. From figures 8 and 9 and table III, one can see that

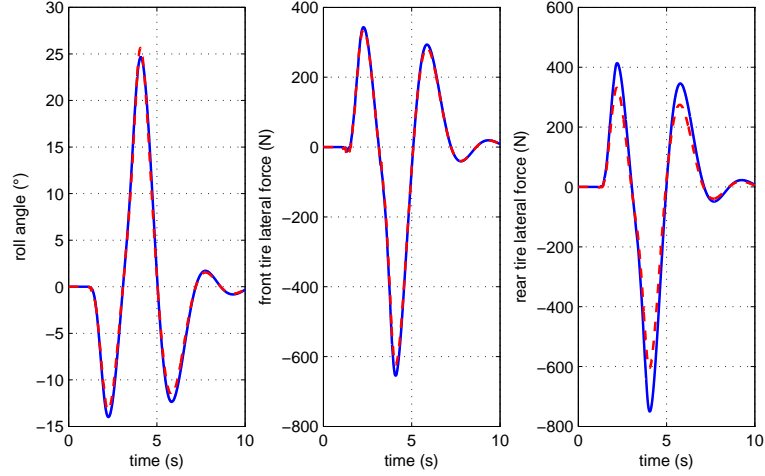


Fig. 7. Double lane change at  $100\text{km/h}$ . In blue: nonlinear multibody model with vehicle's mass increased by 17% and caster angle decreased by 10%, in red: estimation results

the observer gives the better estimation for the case where  $\beta = 0.85$  where the maximal values of the normalized errors are the lowest. However, even with variations of the road adherence, the means and the variances of these errors are always lower than 4% which confirms the robustness of the observer to road friction variations.

TABLE III

NORMALIZED ERROR FOR A DOUBLE LANE CHANGE AND DIFFERENT ROAD ADHERENCE PROFILES. (A)  $\beta = 0.85$ , (B)  $\beta$  VARIES FROM 1 TO 0.7, (C)  $\beta$  VARIES FROM 0.7 TO 0.4

	roll angle			front lateral force			rear lateral force		
	(A)	(B)	(C)	(A)	(B)	(C)	(A)	(B)	(C)
$\max(\epsilon_z)$ (%)	5.42	7.88	12.14	12.87	14.94	16.54	8.57	8.66	8.95
$\text{mean}(\epsilon_z)$ (%)	1.49	1.51	1.59	3.06	3.79	3.81	1.91	2.54	3.81
$\text{std}(\epsilon_z)$ (%)	1.52	1.55	1.72	3.58	4.15	3.25	2.23	2.71	3.49

For the double lane change, the final scenario considered is with a high deceleration of the motorbike ( $-0.5g$ ) which is accompanied with a strong deformation of the suspension. The rider decelerates from  $100\text{km/h}$  to  $10\text{km/h}$  in  $6s$ . The results of simulation of this case are given in the figure 10. In this case, the assumptions considered for modeling are largely violated. There is a high transfer of mass between the two wheels and a strong coupling between the longitudinal and lateral forces. Consequently, the lateral forces are not well estimated, but the ISS performances are still guaranteed and the estimation

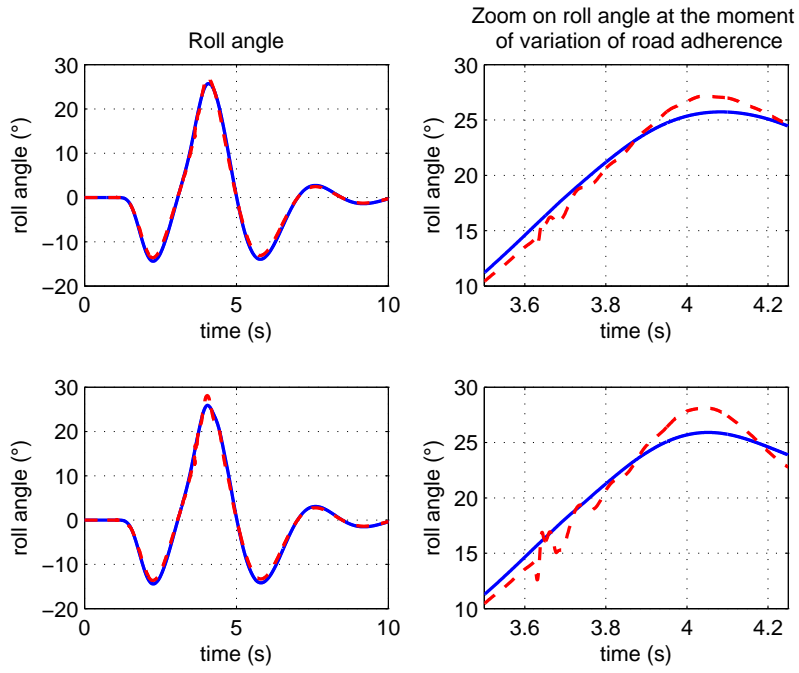


Fig. 8. Double lane change at  $100\text{km/h}$  with change in road friction coefficient. In blue: nonlinear multibody model; and in red: estimation results. Above: first case. Below: second case.

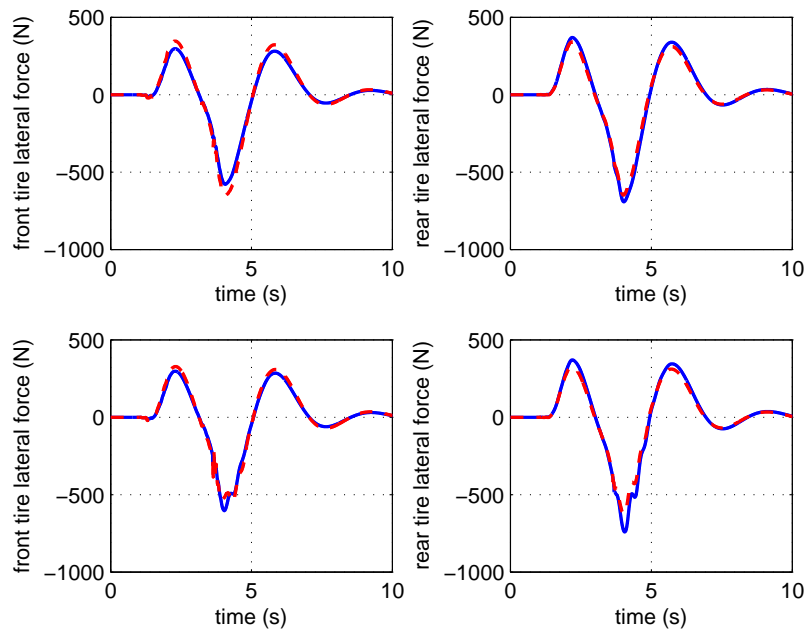


Fig. 9. Double lane change at  $100\text{km/h}$  with change in road friction coefficient. In blue: nonlinear multibody model; and in red: estimation results. Above: first case. Below: second case.

of the roll angle is right.

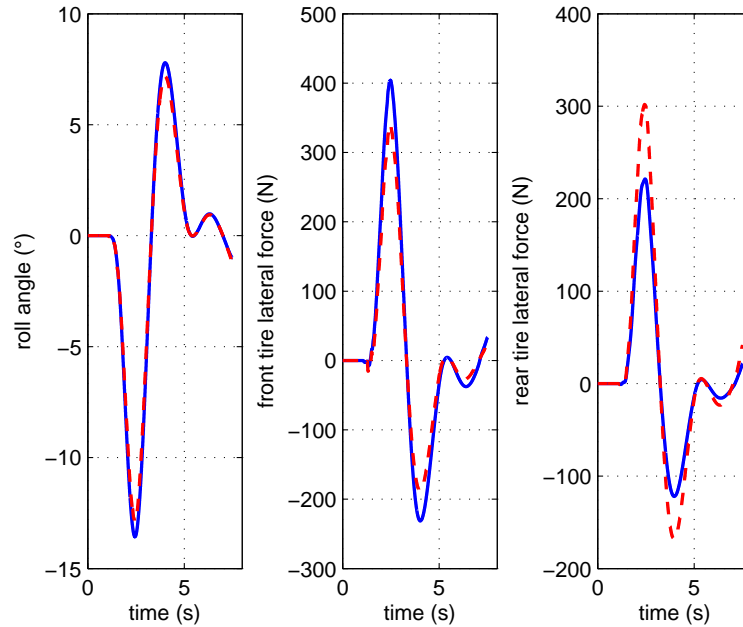


Fig. 10. Double lane change with a high deceleration. In blue: nonlinear multibody model, and in red: estimation results.

The final test is carried out in a traffic scenario where the longitudinal velocity varies between  $30\text{km/h}$  and  $90\text{km/h}$ . To assess the observer in the presence of measurement noise, it is assumed that the measurement signals are affected by centered and random noises with magnitude of 5% of the maximal value of the measured variables. Moreover, to take into account the effect of the roll angle on the measure of accelerations and angular rates, realistic sensors giving the acceleration and the angular rates in the body-fixed frame of the vehicle are considered. In addition, to study the influence of unevenness of the road on the observer accuracy, the elevation and the banking of the road are considered variables. Their graphs are given in figure 11. The results of simulation are given in figures 12 and 13. From these figures, good results may be seen for roll angle and lateral forces estimations for a realistic scenario with different velocities and unevenness of the road.

One of the questions that should be asked about these results is: are the tires nonlinearities excited in this scenario? To answer this question, figure 14 shows the normalized lateral forces as function of rear side-slip angle and front and rear camber angles (the effect of front side-slip angle is not shown because it is negligible in this scenario). From figure 14, it is visible that this scenario does not excite the tire's nonlinearities. But at the same time, these nonlinearities have not been taken into account in the observer design. One of the perspectives for future works is to propose an observer that takes

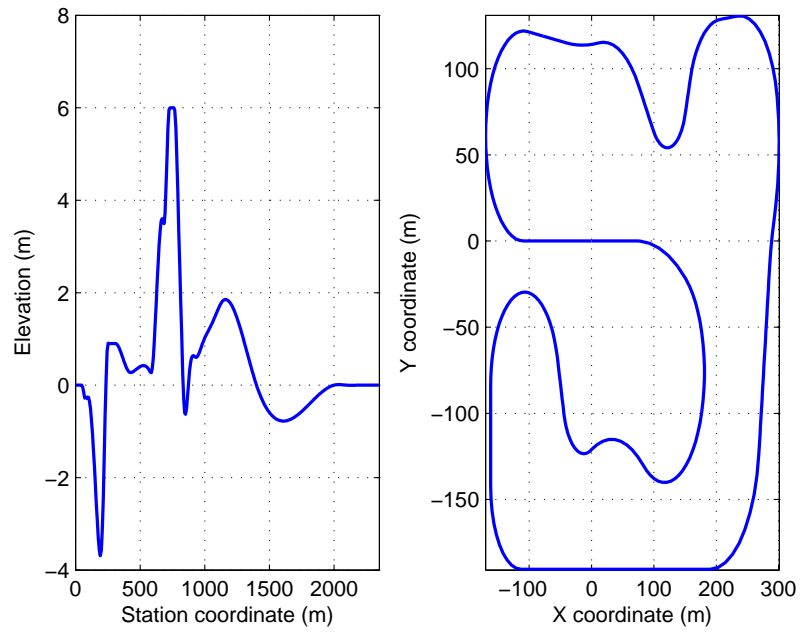


Fig. 11. A traffic scenario of 3km. Left: centerline elevation. Right: centerline trajectory

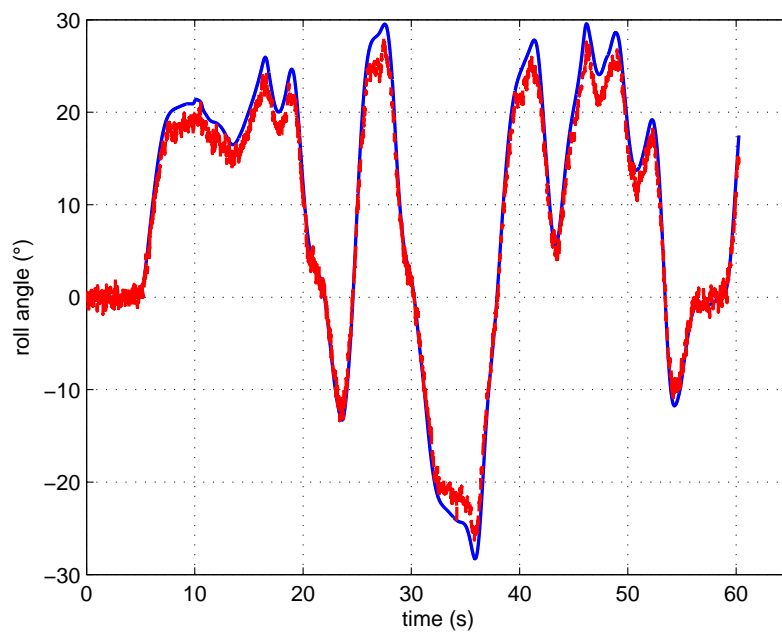


Fig. 12. A traffic scenario of 3km. In blue: nonlinear multibody roll angle, in red: estimation of the roll angle

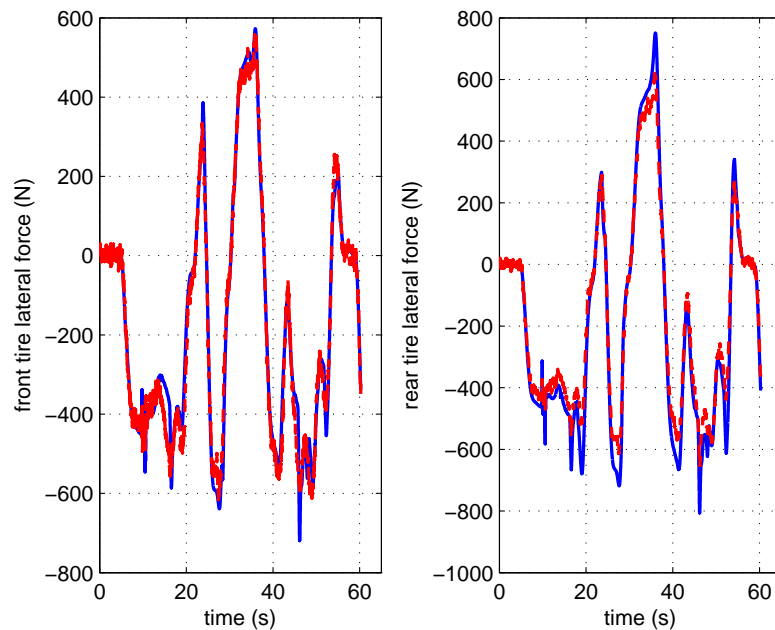


Fig. 13. A traffic scenario of  $3km$ . In blue: nonlinear multibody lateral forces, in red: estimation of the lateral forces

into account these nonlinearities. In this new case, a quasi-LPV model (equation (10)) with more than 2 varying parameters (equation (11)) should be obtained. But, there should be no certainty on the feasibility of the LMI problem.

*Remark 5:* Since the estimation of the lateral forces has never been addressed and tested on a real platform or on a multibody simulator for different longitudinal velocities, only roll angle estimation performances are discussed and compared with some other works. To this end, the root mean squared error (RMSE) is used to compare the roll angle estimation performances of the proposed work with the results obtained in [34]. The results are summarized in the table IV.

TABLE IV  
RMSE RESULTS FOR THE ESTIMATION OF THE ROLL ANGLE.

method	RMSE
Vision system	2.24
IMU - Kalman filter	2.01
Mean vision/IMU	1.20
Proposed observer with ideal sensors	1.28
Proposed observer with realistic sensors	1.85

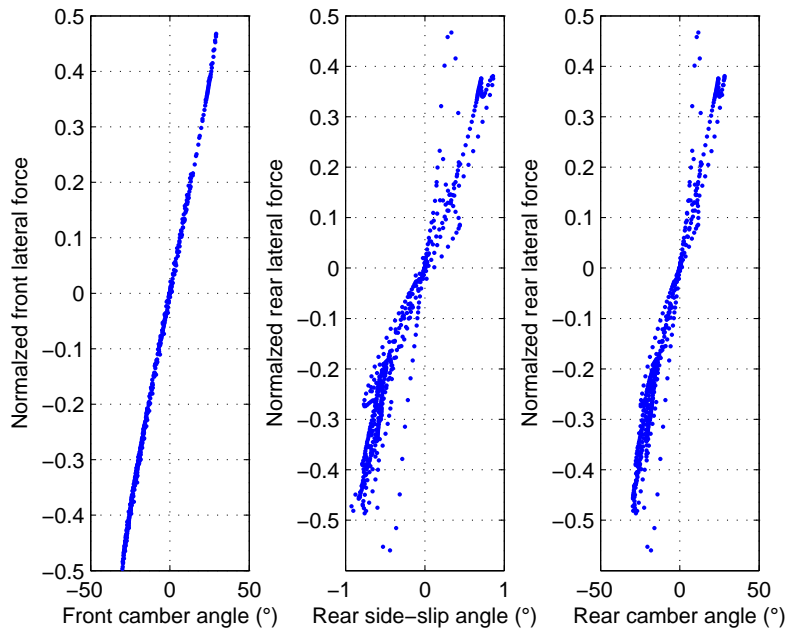


Fig. 14. (Left) Front lateral force vs. front camber angle. (Medium) Rear lateral force vs. rear side-slip angle. (Medium) Rear lateral force vs. rear camber angle.

From the RMSE results, it is seen that the performances of the proposed observer are nearly the same to the combined vision/Inertial Measurement Unit (IMU) method proposed in [34] if the lateral acceleration and the angular rates are exactly known. In the case of realistic sensors with no prior treatment, the estimation of the roll angle remains better than the two first methods. The main advantage of the proposed UI observer is the no-need of a vision system required in [34]. Moreover, in addition to the roll angle, the proposed observer allows also the good estimation of the lateral forces.

## 5. CONCLUSION

The present paper deals with the estimation of the lateral dynamics of motorcycles not for specific longitudinal velocities but for a wide range of forward velocities. Firstly, the quasi-LPV model is simplified to a TS model. Then, a Takagi-Sugeno Unknown Input nonlinear observer is proposed to estimate the motorcycle lateral dynamics. The proof of convergence is guaranteed for a wide range of longitudinal velocities.

Simulations are carried out on a nonlinear multibody model and the results are good for several scenarios and even when the longitudinal velocity or the motorcycle's parameters are not well known. The proposed observer gives an interesting economic solution because it allows the estimation of the

roll angle with only an Inertial Measurement Unit and an optical encoder. Another technical solution proposed in this paper is the estimation of the lateral forces which are very hard to measure.

In future works, it is interesting to include additional available sensors like vision sensors to improve the obtained results. Another perspective is to take into account the geometry of the road which has been considered flat in this paper.

#### ACKNOWLEDGMENTS

This work has been supported by *Evry Val d'Essonne University (UEVE)* and *Informatique, Biologie Intgrative et Systmes Complexes Laboratory (IBISC)*. Thanks are due to Lamri Nehaoua, for enlightening discussions on the modeling of motorcycles.

#### APPENDIX

TABLE V  
NUMERICAL VALUES OF SHARP'S MOTORCYCLE MODEL

Numerical values
$M = 274.4$ , $e_{34} = 61.97$ , $e_{35} = -157.5$ , $e_{36} = 1.458$ , $e_{44} = 71.8$ , $e_{45} = -29.3$ , $e_{46} = 1.391$ , $e_{55} = 122.1$ $e_{56} = -1.496$ , $e_{66} = 0.543$ , $a_{34} = -274.4$ , $a_{44} = -61.96$ , $a_{45} = -3.87$ , $a_{46} = 0.679$ , $a_{47} = 0.95$ $a_{48} = -0.42$ , $a_{51} = 1545$ , $a_{52} = -89.8$ , $a_{54} = 161.4$ , $a_{56} = 1.567$ , $a_{61} = -89.8$ $a_{62} = 36.53$ , $a_{64} = -2.136$ , $a_{65} = -1.525$ , $a_{66} = -12.67$ , $a_{67} = -0.0489$ , $a_{71} = -5282$ $a_{72} = 104503$ , $a_{73} = -112042$ , $a_{74} = -106440$ , $a_{76} = 5481$ , $a_{77} = -5$ , $a_{81} = -2592$ , $a_{83} = -88283$ $a_{84} = 37078$ , $a_{88} = -5$

#### REFERENCES

- [1] ONISR, "L'accidentologie routièrre en 2013," Observatoire National Interministériel de la Sécurité Routièrre, Tech. Rep., 2014.
- [2] B. Evangelos, "Saferider project," French National Agency of Reaserch, Tech. Rep., 2010.
- [3] N. Haworth, P. Rowden, B. Watson, D. Wishart, L. Buckley, and K. Greig, "Motorcycle rider safety project," The Centre for Accident Research & Road Safety Queensland, Tech. Rep., 2012.
- [4] R. Sharp, S. Evangelou, and D. Limebeer, "Advances in the modelling of motorcycle dynamics," *Multibody System Dynamics*, vol. 12, pp. 251 – 283, 2004.
- [5] V. Cossalter, *Motorcycle Dynamics*. Lulu. com, 2006.
- [6] V. Cossalter, M. D. Lio, and F. Biral, "Evaluation of motorcycle maneuverability with the optimal maneuver method," *SAE transactions*, vol. 107, pp. 2512 – 2518, 1998.

- [7] R. Sharp, "Rider control of a motorcycle near to its cornering limits," *Vehicle System Dynamics*, vol. 50, pp. 1193 – 1208, 2012.
- [8] H. Slimi, H. Arioui, L. Nouveliere, and S. Mammar, "Motorcycle speed profile in cornering situation," in *Proc. of the IEEE American Control Conference*, 2010.
- [9] S. M. Savaresi, C. Spelta, A. Moneta, F. Tosi, L. Fabbri, and L. Nardo, "Semi-active control strategies for high-performance motorcycle," in *Proc. of the International Federation of Automatic Control World Congress*, 2008.
- [10] H. Slimi, "Système d'assistance à la conduite pour véhicules à deux-roues motorisés," Ph.D. dissertation, Université d'Evry-Val d'Essonne, 2012.
- [11] L. Gasbarro, A. Beghi, R. Frezza, F. Nori, and C. Spagnol, "Motorcycle trajectory reconstruction by integration of vision and MEMS accelerometers," in *Conference on Decision and Control*, 2004.
- [12] I. Boniolo, S. M. Savaresi, and M. Tanelli, "Roll angle estimation in two-wheeled vehicles," *Control Theory Applications, IET*, vol. 3, no. 1, pp. 20–32, 2009.
- [13] M. Schlipfing, J. Schepanek, and J. Salmen, "Video-based roll angle estimation for two-wheeled vehicles," in *Proc. of the IEEE Intelligent Vehicles Symposium*, 2011.
- [14] A. P. Teerhuis and S. T. H. Jansen, "Motorcycle state estimation for lateral dynamics," *Vehicle System Dynamics*, vol. 50, no. 8, pp. 1261–1276, 2012.
- [15] R. Lot, V. Cossalter, and M. Massaro, "Real-time roll angle estimation for two-wheeled vehicles," in *Proc. of the ASME Conference on Engineering Systems Design And Analysis*, 2012.
- [16] C. Chabane, D. Ichalal, H. Arioui, and S. Mammar, "Proportional two integral (P2I) observer synthesis for single track vehicle," in *International Conference on Systems and Control*, 2012.
- [17] D. Ichalal, C. Chabane, H. Arioui, and S. Mammar, "Estimation de la dynamique latérale pour véhicules à deux roues motorisés," in *Septième Conférence Internationale Francophone d'Automatique*, 2012.
- [18] P. De Filippi, M. Corno, M. Tanelli, and S. Savaresi, "Single-sensor control strategies for semi-active steering damper control in two-wheeled vehicles," *Vehicular Technology, IEEE Transactions on*, vol. 61, no. 2, pp. 813–820, 2011.
- [19] M. Corno, G. Panzani, and S. Savaresi, "Traction-control-oriented state estimation for motorcycles," *Control Systems Technology, IEEE Transactions on*, vol. 21, no. 6, pp. 2400–2407, Nov 2013.
- [20] L. Nehaoua, D. Ichalal, H. Arioui, J. Davila, S. Mammar, and L. Fridman, "An unknown input HOSM approach to estimate lean and steering motorcycle dynamics," *Vehicular Technology, IEEE Transactions on*, 2013.
- [21] M. E. H. Dabladji, D. Ichalal, H. Arioui, and S. Mammar, "Observer based controller for single track vehicles," in *proc. of the IEEE Conference on Decision and Control*, 2013.
- [22] K. Tanaka and H. Wang, *Fuzzy control systems design and analysis: A Linear Matrix Inequality approach*. John Wiley and Sons, 2001.
- [23] D. Ichalal, M. E. H. Dabladji, H. Arioui, and S. Mammar, "Observer design for motorcycle lean and steering dynamics estimation: a Takagi-Sugeno approach," in *proc. of the IEEE American Control Conference*, 2013.
- [24] R. S. Sharp, "The stability and control of motorcycles," *Mechanical Engineering Science*, vol. 13, no. 5, pp. 316 – 329, 1971.
- [25] H. Pacejka, *Tire and Vehicle Dynamics*. SAE International, 2005.
- [26] C. Briat, *LPV & Time-Delay Systems – Analysis, Observation, Filtering & Control*. Springer-Heidelberg, Germany, 2015, vol. 3.
- [27] D. Ichalal and S. Mammar, "On unknown input observers for LPV systems," *Industrial Electronics, IEEE Transactions on*, vol. 62, no. 9, pp. 5870–5880, Sept 2015.

- [28] H. Shim and D. Liberzon, "Nonlinear observers robust to measurement disturbances in an ISS sense," *IEEE Trans. Automat. Control*, 2014.
- [29] E. D. Sontag and Y. Wang, "On characterizations of the input-to-state stability property," *Systems & Control Letters*, vol. 24, no. 5, pp. 351 – 359, 1995.
- [30] Z. Jiang, A. Teel, and L. Praly, "Small gain theorem for ISS systems and applications," *Mathematics of Control, Signals and Systems*, vol. 7, no. 2, pp. 95 – 120, 1994.
- [31] M. Darouach, M. Zasadzinski, and S. J. Xu, "Full-order observers for linear systems with unknown inputs," *IEEE transactions on automatic control*, vol. 39, no. 3, pp. 606–609, 1994.
- [32] D. Ichalal, B. Marx, J. Ragot, and D. Maquin, "Simultaneous state and unknown inputs estimation with PI and PMI observers for Takagi Sugeno model with unmeasurable premise variables," in *proc. of the IEEE Mediterranean Conference on Control and Automation*, 2009, pp. 353–358.
- [33] J. Stephant, A. Charara, and D. Meizel, "Evaluation of a sliding mode observer for vehicle sideslip angle," *Control Engineering Practice*, vol. 15, no. 7, pp. 803–812, 2007.
- [34] M. Schlipfing, J. Salmen, B. Lattke, K. Schroter, and H. Winner, "Roll angle estimation for motorcycles: Comparing video and inertial sensor approaches," in *Intelligent Vehicles Symposium (IV), 2012 IEEE*. IEEE, 2012, pp. 500–505.